

Examination of Fe-Mn Oxide Coating Accretion on Artificial Substrates using LA-ICP-MS

Sheldon R. Huelin^a, Henry P. Longerich^{a*}, Derek H.C. Wilton^a and Brian J. Fryer^b

Contribution from: ^aDepartment of Earth Sciences, Memorial University of Newfoundland, St. John's, NL A1B 3X5, Canada; ^bDepartment of Earth Sciences, University of Windsor, Windsor, Ontario, Canada.

Received: September 9, 2004

Accepted (in revised form): December 22, 2004

Résumé

L'accrétion de couches d'oxyde de Fe-Mn fut examinée sur des substrats artificiels (plaques de porcelaine, ciment, cailloux polis) placés dans la rivière Rennies, à St. John's, Terre-Neuve. Au total, 7 sites d'échantillonnage furent sélectionnés pour la formation d'oxyde de Fe-Mn, les échantillons étant prélevés tous les 3 mois. Des échantillons d'eau furent prélevés le long du bord des substrats et leur pH, oxygène dissout (mg/L) et température furent mesurés; ils furent aussi analysés par ICP-MS (spectrométrie de masse à plasma à couplage inductif) pour 46 éléments. Les concentrations dans la couche d'oxyde de Fe-Mn furent déterminées par LA-ICP-MS (ablation laser avec ICP-MS).

Après optimisation des conditions d'opération de LA-ICP-MS, les données furent acquises avec des temps d'analyse d'environ 2 minutes. La grande quantité de données d'oxyde de Fe-Mn obtenue fut analysée au moyen de statistiques multidimensionnelles, par analyse en composantes principales. Ceci résulte en 2 facteurs, et un graphique des comptes de chaque facteur mena à quatre regroupements des échantillons selon leur emplacement et leur moment d'échantillonnage. Le premier groupe contenait tous les échantillons pris de SJS6B qui était prévu d'être le plus pollué dans cette zone d'étude; après examen des données venant des eaux, il n'en était pas de même. Les couches ici avaient la plus grande quantité de Fe₂O₃ de toute

l'étude, et aussi les plus basses concentrations d'analytes en comparaison aux autres sites d'échantillonnage. Ces niveaux appauvris sont le résultat des grandes quantités de Fe₂O₃.

Le groupe 2 comprenait tous les échantillons prélevés après 3 mois de revêtement d'accrétion. Ils consistaient principalement en Fe₂O₃ et avaient la plus haute teneur d'éléments. Le groupe 3 comprenait les échantillons prélevés après 6 mois de revêtement d'accrétion qui contenaient de plus bas taux de Fe₂O₃, et, conséquemment, de plus grandes quantités de MnO₂; cette tendance se nivela pour le groupe d'échantillons 4 qui furent prélevés après 9 et 12 months de formation. Les concentrations du revêtement ne correspondent pas du tout à aucune des tendances attendues basées sur la chimie du courant d'eau ou les propriétés du revêtement. Elles peuvent être expliquées par un modèle proposé de revêtement d'accrétion qui suggère que de grandes quantités de Fe₂O₃ et de métaux coprécipitaient durant le stade initial de formation du revêtement et que de plus grandes quantités furent adsorbées durant les stades ultérieurs. Il apparaît que les propriétés physiques de Fe₂O₃ amorphe permet la coprécipitation de plus grandes quantités de métaux que MnO₂. La seule exception est Ba, pour lequel une corrélation positive modérée avec MnO₂ fut observée, ce qui peut être relié à son large rayon ionique.

Abstract

Accretion of Fe-Mn oxide coatings was examined on artificial substrates (streak plates, cement,

* Author to whom correspondence should be addressed: henry@esd.mun.ca

polished pebbles) placed in Rennies River, St. John's, Newfoundland. In total, 7 sampling sites were chosen for Fe-Mn oxide formation, and samples were collected every 3 months. Water samples were collected alongside the coating samples, and pH, dissolved oxygen (mg/L), and temperature were measured. The water samples were analyzed by ICP-MS for 46 elements. The Fe-Mn oxide coating concentrations were determined using LA-ICP-MS.

After optimization of the LA-ICP-MS operating conditions, data were acquired with analysis times of approximately two minutes. The large quantity of Fe-Mn oxide data obtained was analyzed with multivariate statistics, in the form of Principal Component Factor Analysis. This produced two Factors, and a plot of the Factor scores led to four groupings of the samples based on location and time of sampling. The first group contained samples taken from SJS6B; this was expected to be the most polluted in this study area, but, after examination of the water data, this did not hold true. Coatings here had the highest amount of Fe_2O_3 for the complete study and also the lowest concentrations of analytes compared to the other sites sampled. These depleted concentrations are a result of the high amount of Fe_2O_3 .

Group 2 consisted of all samples taken after three months of coating accretion. These were mostly all Fe_2O_3 and had the highest concentration of elements. Group 3 was samples taken after six months of coating accretion, and the samples had lower amounts of Fe_2O_3 , and consequently higher amounts of MnO_2 ; this trend levelled off for Group 4 samples, which were those collected after nine and twelve months of formation. Coating concentrations did not match any of the expected trends based on stream chemistry or coating properties. They can be explained by a proposed model of coating accretion that suggests high amounts of Fe_2O_3 and metals coprecipitated for the initial stage of coating formation and greater amounts were adsorbed in the later stages. It appears that the physical properties of amorphous Fe_2O_3 allow higher amounts of metals to coprecipitate than with MnO_2 . The exception to this is Ba, which showed a moderate positive correlation with MnO_2 that may be related to its large ionic radius.

Keywords: Iron-manganese oxides, annual accretion,

LA-ICP-MS, trace metals, principal component factor analysis.

Introduction

Iron-manganese oxide coatings form as thin (< 1 mm), layered structures on fluvial geologic material ranging from silt to boulders (1). The actual coating consists of accumulated iron-manganese oxide layers with a black Mn-oxide phase and a red Fe-oxide phase (2). Iron-manganese oxide coatings also can contain trapped organic material, silt, clay, absorbed water, and living organisms, such as larvae and crustacea (3,4). The Fe-Mn oxides have strong affinities for most elements over a range of pHs, acting as "sponges" for the trapping of heavy metals (5). This enables them to represent stream chemistry and act as geochemical and environmental monitors (3).

Various aspects of Fe-Mn oxide coatings have been studied in the past, including oxide coating accretion. Carpenter and Hayes (6) examined Fe-Mn oxide formation in the Magruder mine area in Lincoln County, Georgia on streak plates. After 36 days, a light-brown Fe-Mn oxide coating indicated the presence of mineralization. Carpenter and Hayes (7) then undertook a similar but more detailed study in Turkey Creek, Georgia. After one year, they found linear growth rates for most elements in the coatings, and the metal/Fe or metal/Mn ratios of coatings on the plates matched or were similar to those on pebbles found in the stream. They found no seasonality in the formation of the coatings, whereas Carpenter *et al.* (8) suggested that there were seasonal differences in coating formation, with possible dissolution occurring from December to March as a result of lower pH and Eh conditions. Cerling and Turner (9) examined accretion of Fe-Mn coatings on gravel and glass plates in a small watershed in eastern Tennessee. Growth only occurred at two of the eight sampling locations; dissolution and abrasion were responsible for loss of the coatings.

Iron-manganese oxide coatings have also been employed in soil and stream sediment surveys for the exploration for porphyry copper, base metal, and gold deposits (10). These, along with the accretion studies, all determined a limited set of elements using partial digestion schemes. Procedures for partial digestions are time-consuming and include steps that are vulnerable to contamination (5). Other problems encountered with dissolution methods are the leaching of analytes from

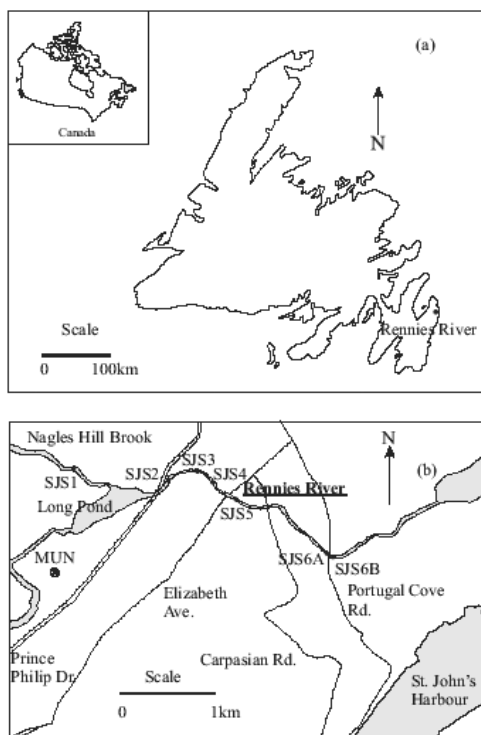


Figure 1. (a) Map of Newfoundland showing study area location; and (b) Rennie's River study area.

the substrate and the resulting high detection limits for some analytes in solution. These, as well as other solution techniques, are also limited to elements which can be satisfactorily maintained in solution.

Laser Ablation-Inductively Coupled Plasma-Mass Spectrometry (LA-ICP-MS) is a microanalytical tool that avoids these problems. It is a low cost, rapid technique with simple sample preparation and typically low detection limits that has been used in the analysis of a variety of geologic samples (11). There has, however, only been limited research on LA-ICP-MS analysis of Fe-Mn oxide coatings. Studies by Coish (12,13) Hale *et al.* (14) and Thompson *et al.* (5) suggested that laser ablation of Fe-Mn oxide coatings could be a viable technique for detecting both mineralized areas and the release of pollutants into fluvial environments. In these studies, however, the absolute concentrations of metals in the coatings were not determined. Ratios of the analyte signals to Fe, Mn, or the sum of Fe and Mn were used, which makes it difficult to compare results between studies. Also, since there were no concentration calculations using a technique such as external calibration with a naturally occurring internal standard, the multiplicative effects of matrix, drift, and quantity of sample ablated in laser ablation were not

corrected (15). There have been no studies completed using LA-ICP-MS to examine Fe-Mn oxide coating accretion as a function of time.

In this study, LA-ICP-MS was used to determine the concentrations of analytes present in Fe-Mn oxide coatings on artificial substrates. Samples were collected on a seasonal basis to determine if there was variable dissolution during the year. This is very important, especially for environmental monitoring, as past contamination events could be erased by dissolution. Multivariate statistics, in the form of Principal Component Factor Analysis (PCFA), were performed on the data to elucidate relationships between the determined trace elements. The results allowed the samples in this study to be separated into distinct groups.

Experimental

Study area

The study area was the Rennie's River system, located in the city of St. John's, Newfoundland and Labrador, Canada (Figure 1). St. John's is a metropolitan area with a population of 150,000 (16). The sampling sites were selected to cover a range of elemental pollution, and it was anticipated that the Fe-Mn oxide coatings would reflect these variations. Seven sampling locations were used. The first sampling site (SJS1) was located in Nagles Hill Brook, which is outside of the built-up metropolitan area and has a maximum width of approximately 1.5 m and average depth of about 0.25 m. It was the least polluted site in this study area. SJS1 flows into Long Pond. Sites SJS2, SJS3, and SJS4 were all located within the metropolitan area drained by the Rennie's River, which flows out of Long Pond. Since sampling sites SJS2, SJS3, and SJS4 are in a more polluted area than SJS1, they were expected to exhibit a different coating composition than site SJS1. The average depth and width for this section of the river is 7 m and 0.50 m, respectively. Site SJS4 is located between Elizabeth Avenue and Carpasian Road, where there are several culverts that contribute dissolved metals to Rennie's River.

The final two sampling sites, SJS6A and SJS6B, are both located further downstream. Site SJS6B is located just below a bridge where a culvert drains a nearby abandoned dump site. Stream bed material in the SJS6B area has a distinct reddish-orange colour, suggesting that an iron-manganese oxide is being produced, whereas, at site SJS6A, the stream bed material has a black colour.

Since both of these sites exist in chemically different environments, there should be obvious differences in the coating accretion and composition even though, spatially, they are not far apart.

Fe-Mn oxide formation setup

Clean artificial substrates were placed in the stream; it was upon these substrates that Fe-Mn oxide coatings were able to “grow.” Three different substrates were used to provide additional information on how different substrates affect coating accretion. Based on previous studies (6,7), conventional streak plates (used for mineralogical tests) were a good choice for a substrate. Polished stream pebbles were chosen based on the fact that this study was focussed on Fe-Mn oxide formation on stream pebbles. Thirdly, cement substrates were used as a Fe-Mn oxide collector. This was following a study by Love and Bailey (17) in which cement substrates were placed in streams and epilithic invertebrates which grew on these materials were examined. To prepare cement substrates, tennis balls were cut in half, filled with cement, and allowed to set, following which the formed concrete was removed from the mould.

Since the chemical environment is known to change with location in the river, it was important that the substrates remain stationary throughout the study. This was done by attaching the substrates to building bricks using GE Silicone Sealant.

Experimental investigations began on February 25, 2002, when the building bricks and attached substrates were placed at midstream in the sampling sites. Eight bricks with attached substrates were placed at each site, with a plan of collecting two sets of substrates every three months for a year, until February 25, 2003. This experimental design was conceived with a goal of determining seasonal variation in the coatings.

Sampling

The Fe-Mn oxide collectors were sampled approximately every three months. The substrates were detached from the bricks and placed in brown paper sampling bags. At the same time, two pebbles from the streambed at each site were also collected. This allowed comparisons between “new” and “old” coatings. All samples were carried to the lab, where they were washed with demineralised water and dried in a HEPA air filtered drying space. After drying, the samples were placed in pre-cleaned Ziploc® resealable containers for later

analysis. These containers were cleaned by rinsing them three times with deionized water and drying them in a HEPA air filtered drying space.

After the pebbles and substrates were cleaned and dried, they were cut with a rock saw. To minimize contamination, water was not used to cool the blade, and the pieces cut from the pebbles were washed with deionized water and air dried after cutting. After drying, they were attached to standard geological thin section glass slides using five minute epoxy. Samples were then placed in a HEPA air filtered drying space located in the Department of Earth Sciences at MUN while the adhesive set.

To accompany the Fe-Mn oxide coating samples and to help understand coating formation, water measurements were taken in the field at each sampling site. These measurements included pH (Orion Model 290A, Boston, MA), dissolved oxygen (Orion Model 835, Boston, MA), and conductivity (Orion Model 835, Boston, MA). Water sampling was repeated at each site approximately every 10 days for one year, starting in February, 2002. The water samples were analysed for 46 elements using ICP-MS. For these samples, at each of the sampling locations, a new BD Luer-Lok™ 30 mL syringe was rinsed with stream water three times and then 100 mL was filtered, using a new Fisherbrand™ 0.45 µm syringe filter, into a pre-cleaned Corning Snap-Seal™ polyethylene bottle. These bottles were previously cleaned by placing them in 8N nitric acid (HNO₃) for a minimum of 24 hours. The bottles were then rinsed three times with deionized water and dried in a HEPA filtered air-drying space. Collected water samples were immediately transported to the lab, where 2 mL of 8M nitric acid (HNO₃) was added. After acidification, the samples were placed in cold storage. Monthly water composites were made in which equal weights of the weekly water samples were combined to form a composite sample.

Water samples data acquisition

Concentrations for 46 analyte elements, ranging from Li to U, were determined using a HP4500+ quadrupole ICP-MS. Operating conditions are in Table 1. This procedure is essentially the same as has been used for years and has been described previously (18). Final sample preparation consisted of taking 1 mL of water from the sample container, placing it in a 12 mL test tube, and diluting to 10 mL with 0.2 M HNO₃. Dilution is by

Table 1. HP4500+ quadrupole ICP-MS operating conditions for water analysis

Plasma Conditions	
RF Power	1250 W
Plasma gas flow	15 L min ⁻¹
Auxiliary gas flow	0.98 L min ⁻¹
Nebulizer gas flow	1 L min ⁻¹
Data Acquisition	
Scanning mode	Single point per peak
Points per mass	1
Acquisition time per mass	10 s
Average settling time	1.8 ms
Average dwell time	100 ms
Masses analyzed	⁶ Li, ⁷ Li, ⁹ Be, ¹⁰ B, ¹² C, ¹⁴ N, ²⁵ Mg, ²⁷ Al, ²⁸ Si, ³¹ P, ³⁴ S, ³⁵ Cl, ⁴² Ca, ⁴³ Ca, ⁴⁹ Ti, ⁵¹ V, ⁵² Cr, ⁵³ Cr, ⁵⁴ Fe, ⁵⁵ Mn, ⁵⁶ Fe, ⁵⁷ Fe, ⁵⁹ Co, ⁶⁰ Ni, ⁶⁵ Cu, ⁶⁶ Zn, ⁷⁵ As, ⁷⁹ Br, ⁸² Se, ⁸⁵ Rb, ⁸⁸ Sr, ⁹⁸ Mo, ¹⁰⁷ Ag, ¹¹¹ Cd, ¹¹⁸ Sn, ¹²¹ Sb, ¹²⁷ I, ¹³³ Cs, ¹³⁷ Ba, ¹³⁹ La, ¹⁴⁰ Ce, ²⁰¹ Hg, ²⁰⁵ Tl, ²⁰⁸ Pb, ²⁰⁹ Bi and ²³⁸ U

weight, and the results are corrected for the calculated dilution.

Reagent blanks were measured to monitor contamination from collection, preparation, and analysis. These blanks comprised deionized water that underwent the same sample preparation as the field samples. Five USGS water reference materials (t129, t137, t143, t145, and t155) were used for quality control. Some field duplicates, replicate samples taken at the same sampling point, and split samples, field samples that were divided into two aliquots in the laboratory, were also measured. Field blanks were also measured; these consisted of deionized water that was “sampled” in the field and underwent the same sample preparation as other field samples. After data acquisition, concentrations were calculated using an in house waters package that was developed at Memorial University of Newfoundland (19). Finally, values obtained from field blanks were subtracted from measured field sample concentrations.

LA-ICP-MS data acquisition

For the pebble chips, two chips from each pebble were analysed. Due to analysis time constraints, samples for the 3, 6, and 9 month periods from sites SJS2, SJS3, SJS4, and SJS5 were not analyzed. In previous work, individual spots were analysed on the coatings, but the disadvantage of this procedure is that the coatings are heterogenous,

with significant variations in the same coating (12,13). In this work, a traverse was used; this should give a better sample of the coating composition because it is, in effect, a series of points along a line on the chip.

Analyses of the pebble coatings were completed at the Great Lakes Institute for Environmental Research at the University of Windsor, Windsor, Ontario, Canada. The laser used for the Fe-Mn oxide analysis was a non-homogenized, high power (~1.0 mJ/pulse), frequency quadrupled (266 nm), Continuum® (Santa Clara, CA) Surelite® I Nd-YAG laser. The laser optics system was designed by Brian J. Fryer and the Metals Research Laboratory of the Great Lakes Institute for Environmental Research (GLIER) and the Department of Earth Sciences at the University of Windsor. Further details on the optics system can be found in Crowe *et al.* (20).

Samples were placed in a custom-designed cell that was fabricated from a Lexan cylinder with a screw-top removable lid and a fused silica window. When samples are in the form of standard thin sections, the cell has a volume of 100 mL. Ablation carries material from the sample cell to the ICP-MS via a length of 4 mm i.d. plastic tubing. The ablated material was then transported to a standard Thermo Elemental® ICP torch by a mixture of ultra-pure nebuliser Ar gas (BOC®, Windsor) and N₂ gas (BOC®, Windsor). Introduction of the N₂ to the Ar gas was done prior to its entering the sample cell using an Aridus® micro-concentric desolvating nebuliser gas controller. The ratio of Ar to N₂ was 50:1, which gave maximum sensitivity. LA-ICP-MS analysis of the samples was observed using a Sony analog camera interfaced to a PC through a video capture card.

The ICP-MS was a Thermo Elemental® X-7 (Windsford, UK) quadrupole instrument. This is a high sensitivity instrument (450 million cps ppm⁻¹ at U) using conventional solution nebulisation that gives relatively low backgrounds (*i. e.* 400 cps for ⁵⁷Fe) and has a dual (analogue and digital) mode detector system. This MS also offers fast switching between different resolution, giving an additional means (the use of high resolution) of reducing signals for elements present at high concentrations.

LA-ICP-MS optimization

Initial studies indicated elevated concentrations of Al₂O₃ and SiO₂ were present, and, with visual observation using a low-powered microscope, it was clear that, in addition to the Mn-Fe oxide coating, the substrate was

Table 2. LA-ICP-MS operating conditions

Laser	
Model	Continuum Surelite I®
Wavelength	266 nm
Aperture diameter	2.5 mm
Energy per pulse	0.45 mJ
Repetition rate	20 Hz
Micro-concentric desolvating nebulizer	
Model	Cetac Aridus®
Temperature	70 °C
Ar gas flow	2.96 L min ⁻¹
N ₂ gas flow	17 mL min ⁻¹
ICP-MS Plasma Conditions	
RF power	1280 W
Plasma gas flow	15 L min ⁻¹
Auxiliary gas flow	1.02 L min ⁻¹
Nebulizer gas flow	1.05 L min ⁻¹
Data acquisition	
Scanning mode	Rapid peak hop
Dwell time	10 ms
Points per peak	1
Settling time (average)	2.13 ms
Masses analyzed (*indicates data acquired in high resolution mode)	²⁷ Al*, ²⁹ Si*, ⁴³ Ca*, ⁴⁷ Ti, ⁵¹ V, ⁵³ Cr, ⁵⁵ Mn*, ⁵⁷ Fe*, ⁵⁹ Co, ⁶² Ni, ⁶⁵ Cu, ⁶⁶ Zn, ⁷⁵ As, ⁸² Se, ⁸⁶ Sr, ⁸⁹ Y, ¹⁰⁷ Ag, ¹¹¹ Cd, ¹¹⁸ Sn, ¹³⁷ Ba, ¹³⁹ La, ¹⁴⁰ Ce, ¹⁹⁷ Au, ²⁰² Hg, ²⁰⁶ Pb, ²⁰⁷ Pb, ²⁰⁸ Pb, ²⁰⁹ Bi, ²³² Th and ²³⁸ U

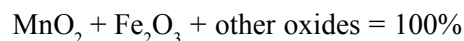
also being sampled by the laser. This required adjustment of the laser power (adjustable between 0 and 0.45 mJ pulse⁻¹) and focus position. As the focus position is raised, the defocused beam produces a larger diameter beam, and thus a larger ablated sample area, but, due to the lower energy density, the beam does not penetrate into the sample as quickly. Defocussing of the beam also decreases the change of the beam diameter with pit depth. Utilization of a ½ waveplate to reduce power (to 0.05 mJ pulse⁻¹) and focal height (to 400 μm above the sample surface) resulted in a laser energy density of 2.55 Jcm⁻² and ablation pits with a diameter of 50 μm. This resulted in low concentrations of Al₂O₃ and SiO₂, indicating minimal ablation of the substrate.

Operating conditions for the LA-ICP-MS analysis are given in Table 2. After a sample was placed in the sample

cell, the cell was allowed to flush for approximately 10 minutes in order to remove residual atmospheric gases. Each run began with two SRM 610 (National Institute of Science and Technology, NIST) acquisitions, followed by analysis of the samples (8-16 analyses) and then a repeat of two SRM 610 acquisitions. This SRM material is considered homogeneous (~1%) for many trace elements (21). Each acquisition started with approximately 60 s of background. During this time, data were collected with the beam blocked but with the laser firing. After the 60 s background, the laser beam was unblocked. Line rasters were used for each acquisition, including the NIST 610 reference material. For the Fe-Mn oxide coating samples, pebble locations with thicker and more even coatings were selected. Both the reference material and samples were ablated for 60 seconds. There was also some depth profiling analysis, in which the laser was turned on and allowed to ablate the Fe-Mn oxide coating at a single spot to obtain information on the coating depth and the variations of analyte concentrations with depth.

LA-ICP-MS data reduction

The program CONVERT was used to reformat ICP-MS instrument software data into a common format for use by LAMTRACE (22). The converted files (maximum of 20) were introduced into the LAMTRACE data reduction program, where signal (cps) versus time graphs were produced. For each element, the mean background was subtracted from the mean gross analyte ablation count rates to produce net count rates. The integration window for the background and the analyte are selected by the program, with subsequent adjustment by the operator if needed. LAMTRACE then calculated the mean net signal as the difference between the mean gross analyte intensity and the mean background intensity (cps). Concentrations of selected elements were then calculated based on the known NIST 610 concentrations and concentrations of the internal standard. The assumed chemical composition of the major element oxide phases in Fe-Mn oxide coatings are MnO₂ and Fe₂O₃ (8,23,24,25). In this work, for internal standardization, the assumption that:



was used. It has been suggested that at least 99% of the oxides present on these coatings are phases of Fe and

Mn (7).

In the LAMTRACE program, one element is initially selected as the internal standard. In this work, Mn was arbitrarily chosen as the internal standard, with a concentration of 81.599% MnO (equivalent to 100% MnO₂) in the coating. LAMTRACE calculates Fe concentrations as FeO, which were converted to Fe₂O₃. The two oxides (Mn and Fe) were then summed to produce a MnO₂ + Fe₂O₃ value, and the data were initially normalised to this value. Examination of the data revealed that the total concentration of all elements was routinely above 100%, and thus further normalisation was performed on the data. Trace element concentrations were converted to their corresponding oxides value: V₂O₅, Cr₂O₃, CoO, NiO, CuO, ZnO, As₂O₅, SeO₃, SrO, Y₂O₃, Ag₂O, CdO, SnO₂, BaO, La₂O₃, CeO₂, Au₂O₃, HgO, PbO, Bi₂O₃, ThO₂, and UO₃. These concentrations, along with MnO₂ and Fe₂O₃, were added together, and the original concentrations were divided by this value to normalise the data. Three oxides, Al₂O₃, SiO₂, and TiO₂, were eliminated from the normalisation because the substrate was frequently sampled, and this led to elevated and random values for these three oxides.

Results and Discussion

Statistical analysis

Before statistical analysis was carried out, some analytes were removed from the data sets. For the water data, the elements Be, B, P, S, Br, Se, Hg, and Bi were omitted from further consideration because most values were below detection limits. The parameter set used for the water analysis includes multiple isotopes for selected elements; this allows for the selection of the isotope which is optimal for a given sample type when considering the background and interferences. For this study, when more than one isotope is acquired, the following isotopes were selected: ⁷Li, ⁴³Ca, ⁵³Cr, ⁵⁷Fe. For the LA-ICP-MS data, Se, Au, and Hg had concentrations below the detection limit and were eliminated from further analysis. Of the three lead isotopes, ²⁰⁸Pb was chosen over ²⁰⁶Pb and ²⁰⁷Pb due to its greater abundance.

Both data sets were log transformed, which made the data more closely approximate a normal distribution. Log-transformation also reduces the extremity of outliers and has a standardising effect by bringing elements of high concentration into a similar range as elements of low concentration. For all values which were greater than

zero, the measured value was used. However since negative and zero values cannot be log-transformed, these were arbitrarily set to ½ of the detection limit (26). In order to visually examine the data, descriptive statistics, in the form of box plots and scatter plots, were created using Minitab® 13.1. Pearson correlation coefficients were used to quantify associations between the analytes. For the water samples, there was a very strong correlation between La and Ce, with a Pearson correlation coefficient of 0.989. Cerium was selected for further data analysis since Ce concentrations were, as expected, higher than La in all determinations. For the LA-ICP-MS data, Y and La had a strong correlation coefficient of 0.946. Examination of the scatter plot showed that the points followed an excellent correlation. It was decided that La would be eliminated because it showed strong correlations with both Y and Ce.

The LA-ICP-MS data set contained a large number of variables, and relationships between the elements and Fe-Mn oxide coating are not well understood. In order to derive meaningful information from both, variable grouping was used. Principal Component Factor Analysis (PCFA), also known as Principal Component Analysis (PCA), was carried out on the data. This reduces a large number of variables into a smaller set of dimensions by analysing how the variables are interrelated (27). Factors (PCFA) or components (PCA) are produced that account for more of the variance than any other combination. For each Factor, a loading is calculated for each variable. The absolute value of the loading indicates how much the variable contributes to the Factor, with values ranging from 0 to ± 1, the sign indicates whether the variable is positively or negatively correlated with the component (28). Variables that have a low loading on each Factor were eliminated from subsequent refinement of the PCFA. Eigenvalues were produced; these give the amount of variance accounted for by a particular Factor. To determine how many Factors to retain, the eigenvalues were examined. The number of retained Factors was based on the Kaiser criterion, which states that only Factors having an eigenvalue greater than 1 should be kept (29).

There were five variables that loaded low on all of the factors: Co, As, Ag, Cd, and Sn. Four of these are chalcophile, and Sn is siderophile, but to a lesser extent may be considered lithophile (30). As mentioned above, these chalcophile elements are associated with sulfide ore deposits and are not expected to be found at elevated

Table 3. Factor loadings and eigenvalues from unrotated PCFA for log-transformed element concentrations in the coatings that formed on the artificial substrates.

Variable	Factor 1	Factor 2
logV	-0.878	0.276
logCr	-0.888	0.364
logMn ₂ O ₃	-0.332	-0.862
logFe ₂ O ₃	-0.109	0.934
logNi	-0.882	-0.110
logCu	-0.784	-0.075
logZn	-0.763	-0.036
logSr	-0.836	0.070
logY	-0.897	0.151
logBa	-0.452	-0.810
logCe	-0.798	-0.227
logPb	-0.795	-0.072
logBi	-0.900	0.164
logTh	-0.958	0.036
logU	-0.922	0.032
EigenValue	9.21	2.612
%Variance	0.614	0.174

concentrations in St. John's. Therefore, these should not show any distinguishing properties, either temporal or spatial, in these samples.

Cobalt concentrations in the water samples taken from Rennies River were generally low, with all values less than 1 ppb. Concentrations in the polluted sites, SJWS2-SJWS6B, were only slightly higher than unpolluted, and therefore anthropogenic inputs were minor. The Co concentrations determined by LA-ICP-MS were generally high, but RSD values were also high.

Arsenic concentrations in the water samples were generally low, with values less than 1 ppb. This was expected, again due to the absence of sulphide minerals in the study area. Concentrations in the polluted sites were only slightly higher than in the "pristine" site. Concentrations in the Fe-Mn oxide coatings were generally low, with small differences between concentrations in samples. For Ag, Cd, and Sn,

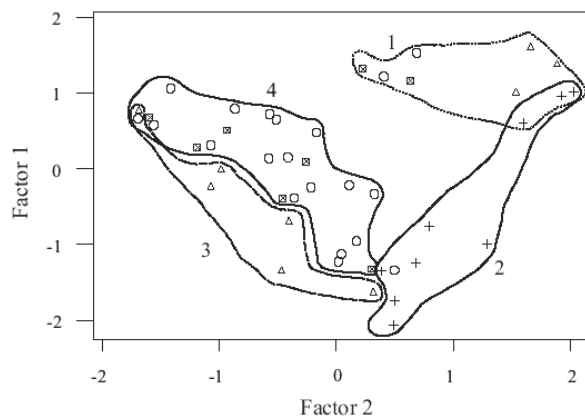


Figure 2. Plot of Factor 1 versus Factor 2 scores obtained from PCFA of elements in Fe-Mn oxide coatings on artificial substrates collected from Rennies River; + after 3 months of coating accretion (Group 2), Δ after 6 months (Group 3), \square after 9 months (Group 4), and \circ after 12 months (Group 4). Group 1 consists of samples taken from site SJS6B.

concentrations in water samples were low for both water samples and Fe-Mn oxide coatings. All three of these also exhibited high RSD values.

Based on the Kaiser criterion, two factors were found to be significant (Table 3). Factor 1 accounted for 61.4% of the variance and had an eigenvalue of 9.21; the variables that loaded high on this factor were V, Cr, Ni, Cu, Zn, Sr, Y, Ce, Pb, Bi, Th, and U. Factor 2 had an eigenvalue of 2.612 and accounted for 17.4% of the variance; variables that loaded high were MnO₂, Fe₂O₃, and Ba.

Rotation of the PCFA data space can be applied in order to make each of the factors more recognizable within the original data set (31). Four types of rotation were tried: Varimax, Quartimax, Equamax, and Orthomax. For regional separation, no rotation gave better groupings for both data sets.

When the Factor 1 versus Factor 2 scores were plotted (Figure 2), the samples could be classed into four groups. Group 1 consisted of samples from all four sampling periods that were taken from SJS6B, group 2 contained all of the samples taken from the 3 month period, group 3 contained the samples that belonged to those sampled from the 6 month period, and group 4 consisted of samples taken from sites that were sampled after 9 and 12 months. Substrate composition appears to have a negligible effect on Fe-Mn oxide formation, since none of these groupings reflected the three different substrates used in the study.

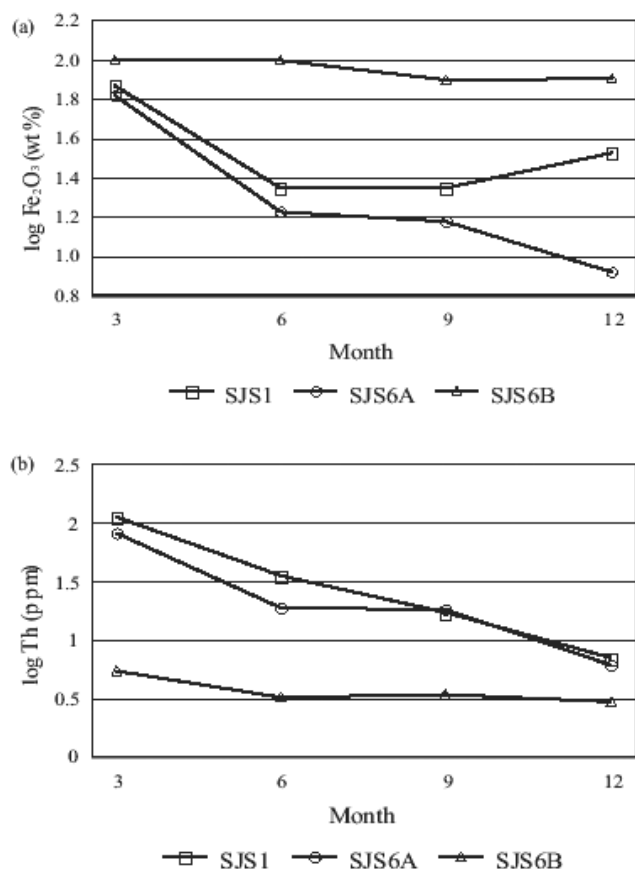


Figure 3. Log-transformed concentrations of (a) Fe_2O_3 (wt%) and (b) Th (ppm) on Fe-Mn oxide coatings accreted on artificial substrates taken from Rennies River sites SJS1, SJS6A, and SJS6B for the period of February 2002 to February 2003.

Fe-Mn oxide coating group 1

Group 1 contained samples from SJS6B, and these were expected to display the highest concentrations of most metals in the water and Fe-Mn oxide coating samples. This is because the sample site is an outflow for Kelly's Brook, which was a natural brook that drained a large residential area and a former city dump (32). Only 5 of the elements (Mn, Fe, Sr, Ba, and U) in the PCFA factors had their greatest concentration at this site. The low number of elements exhibiting elevated concentrations at Kelly's Brook may be explained by noting the fact that the brook flows through a wetland marsh that could have acted as a filter for these pollutants and thus removed them from the water (32). For the analytes that displayed elevated stream water concentrations at site SJS6B, only Fe_2O_3 had elevated coating concentrations (Figure 3a); the remaining elements in both of the PCFA Factors had their lowest concentration at site SJS6B (Figure 3b). It should be noted

that there was insufficient data to include error bars in the figures. Indeed, no acceptable external calibration reference material was available for LA-ICP-MS analysis of Fe-Mn oxide coatings on stream pebbles, thus making correct error bars on the figures unrealistic and discussion of detection limits inappropriate.

Besides the stream water analyte concentration, the Fe-Mn oxide analyte coating concentration is also affected by the pH of the stream environment. As the pH is increased, adsorption of metals onto the Fe-Mn oxide coatings also increases, leading to elevated concentrations (33). This relates to the Fe-Mn oxides zero point of charge (ZPC), which is the pH at which the surface is uncharged (30). For MnO_2 , this occurs at a pH of 3; iron oxides (*i.e.* Fe_2O_3) have a ZPC between 6.5 and 8.5. At higher pH, the Fe-Mn oxide surface will have a larger negative charge, and thus it will be able to adsorb more cations from solution. Of all of the sampling sites in Rennies River, site SJS6B had the highest pH throughout the year, with the pH ranging from 6.89 to 7.56. Adsorption of elements was expected to be favoured at this site, but this was not found.

The low analyte concentrations at site SJS6B may be due to the large amount of Fe_2O_3 . Compared to sites SJS1 and SJS6A, site SJS6B has a Fe_2O_3 -rich coating (Figure 3a), ranging from 74.3% to 99.8% for all determinations over the entire sampling period. At the remaining sites, the amount of Fe_2O_3 ranges from 6.54% to 85.6%. The iron-richness of the SJS6B oxide coatings was observed in accumulation of the Fe-Mn oxides throughout the one year sampling period. After 3 months of coating accretion at all three sites, the coating on all substrates was a red-orange colour. For those samples collected from SJS6B after 6, 9, and 12 months, as the amount of MnO_2 increased, the coating became thicker and became a brown-red colour. For the other sites, the coating became thicker and approached a brownish-black colour. Iron oxides are considered poor adsorbers of elements compared to manganese oxides (30,34). Iron oxides have a higher ZPC than manganese oxides, and therefore they will have a lower negative surface charge than manganese oxides in typical natural stream environments. This reduces their effectiveness for the adsorbance of cations, resulting in low elemental concentrations as observed at site SJS6B.

The amount of Fe_2O_3 decreased with time over the one year sampling period (Figure 3a). This could be related to dissolved oxygen and pH, both of which were

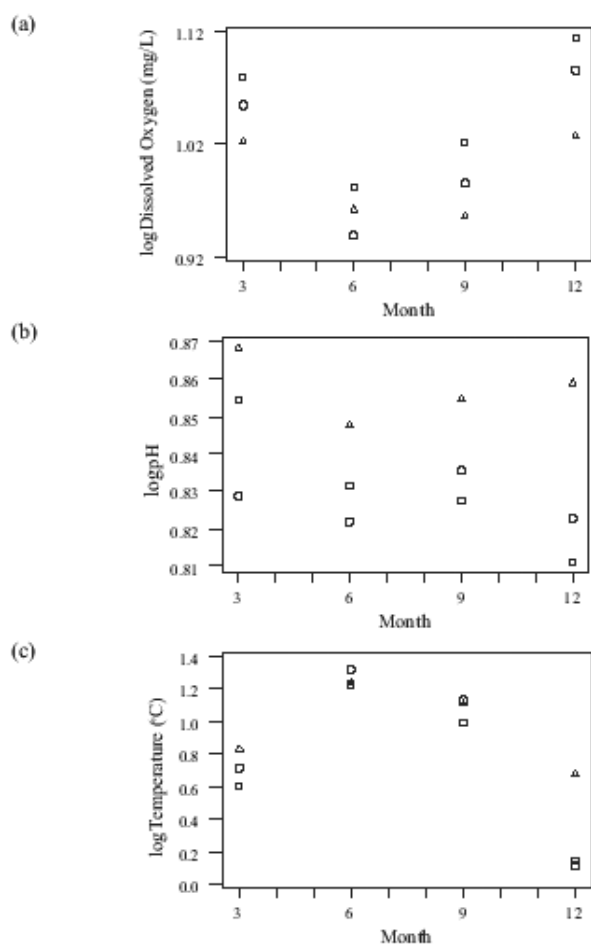


Figure 4. Plot of log transformed values of (a) dissolved oxygen (mg/L), (b) pH, and (c) temperature ($^{\circ}$ C) for samples taken from Rennies River sites SWS1(\square), SWS6A(\circ), and SWS6B(\triangle) over a 1-year period from February 2002 to February 2003.

measured at site SJS6B throughout the sampling period. Dissolved oxygen is important for determining the relative amount of each oxide phase that will form. Low dissolved oxygen prevents the precipitation of MnO_2 , resulting in increased Fe_2O_3 concentrations (34). At site SJS6B, elevated dissolved oxygen values occurred for the first 3 months (Figure 4a), and thus MnO_2 formation should have been favoured at this sampling period. The pH values also determine which oxide phase is formed. Iron oxides precipitate at pH values greater than 4.5, whereas manganese oxides require values greater than 8 (35). Oxidation rates of both iron and manganese increase by a factor of 100 for each pH unit increase, with manganese requiring a much higher pH for equivalent rates of oxidation (36). At site SJS6B, pH values are highest after 3 months of coating accretion, thus favouring MnO_2 precipitation (Figure 4b). Thus, the high amounts

of Fe_2O_3 must be related to some other factor.

The trend of decreasing amounts of Fe_2O_3 at the SJS6B site may be explained by the mechanism that involves the surface of the precipitated Fe_2O_3 particles providing an area for MnO_2 precipitation (9,37,38,39). As the Fe_2O_3 accumulates on the substrate after 3 months in Rennies River, MnO_2 is able to accumulate, thus leading to higher concentrations of MnO_2 in later months.

For most of the remaining elements in the two factors, samples from SJS6B exhibited the trend of having the highest concentration after 3 months of coating accretion (Figure 3b). It was expected that element trends would follow that of MnO_2 , with increasing concentrations as the coatings aged.

Fe-Mn oxide coating groups 2, 3 and 4

Group 2 was made up of samples collected from sites SJS1, SJS6A, and SJS6B after 3 months of coating accretion. This group is very similar to group 1, in that both groups have a high Fe_2O_3 compositions as observed in the overlap between the two groups (Figure 2). For all three substrates, the amount of Fe_2O_3 in the coatings ranges from 48.6% to 98.8%. Samples collected after 6 months (Group 3) of coating accretion have much lower amounts of Fe_2O_3 (Figure 3a). The appearance of the coating changed from a light brown stain to patches of a brown-black coating. The amount of Fe_2O_3 then remains relatively constant to the termination of the experiment at 12 months (Group 4). The coating becomes thicker and eventually completely covers the surface of the substrate. Again, this suggests that Fe_2O_3 provides a surface for MnO_2 precipitation.

Similar to site SJS6B, accumulation of other elements in the oxide coating is high after 3 months of accretion, even though MnO_2 amounts are low (Figure 5). This was not expected, since manganese oxides are predicted to be a better adsorber of elements than iron oxides (30,34). Pearson correlation coefficients were calculated for all of the elements in Factor 1 and Factor 2 and the MnO_2 and Fe_2O_3 phases for all of the artificial substrate samples collected during the study (Table 4). Barium is the only element that exhibited a strong positive correlation (0.819) with MnO_2 . This relationship is present in Factor 2, with MnO_2 having a negative loading of -0.862 and Ba having a loading of -0.810. Vanadium and Cr showed the strongest relationships with Fe_2O_3 , but even so, the values were only slightly positive. Chromium was expected, since

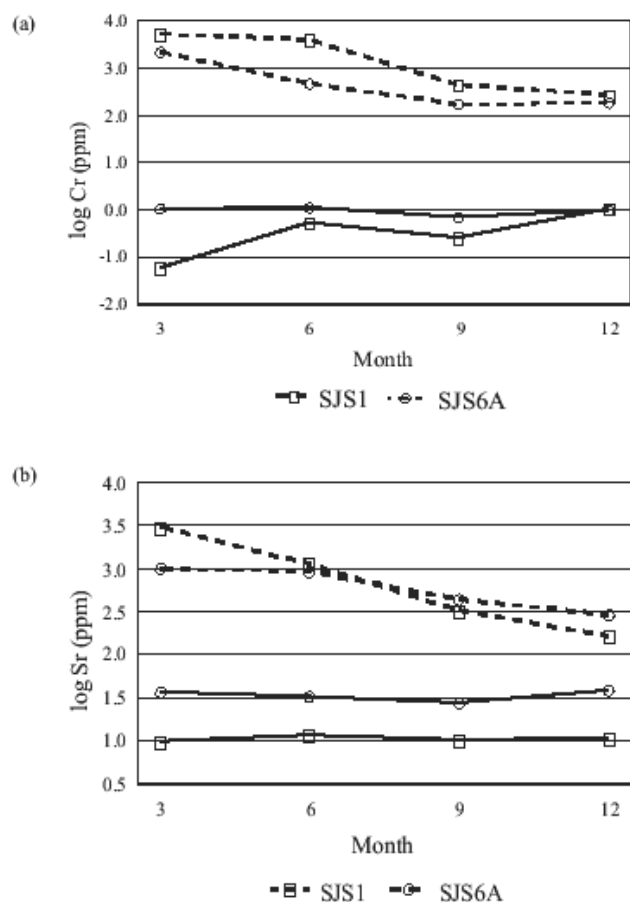


Figure 5. Log-transformed (a) Cr (ppm) and (b) Sr (ppm) concentrations on Fe-Mn oxide coatings (dashed lines) accreted on artificial substrates and water samples (solid lines) taken from Rennies River sites SJS1 and SJS6A for the period of February 2002 to February 2003.

it forms an anion in solution and is strongly adsorbed by the positive surface of Fe_2O_3 . Vanadium, which has a similar ionic radius to Cr, 49.5-68 pm compared to 58 pm, forms HVO_4^{2-} anions that can be strongly sorbed by Fe_2O_3 (40). These results indicate that Fe_2O_3 did not continue to adsorb all of these elements throughout the 12 month study period. Therefore something unique was occurring after 3 months of coating accretion.

Data for the water samples collected from Rennies River were reexamined to understand these element trends. None of the elements in any of the factors showed maximum water concentrations for the 3 month samples; therefore, high Fe-Mn oxide coating concentrations are likely the result of some other variable, such as stream water temperature, dissolved oxygen, or pH.

The adsorption of metals on Fe-Mn oxide coatings increases with temperature (41). Temperature ($^{\circ}\text{C}$)

Table 4. Pearson's-R correlation coefficients calculated between elements in Factor 1 and Factor 2 of the artificial substrate PCFA and MnO_2 and Fe_2O_3 .

Element	MnO_2	Fe_2O_3
V	0.121	0.422
Cr	-0.021	0.430
Ni	0.369	-0.042
Cu	0.273	0.002
Zn	0.314	0.046
Sr	0.121	0.117
Y	0.129	0.190
Ba	0.819	-0.654
Ce	0.408	-0.155
Pb	0.366	0.080
Bi	0.161	0.236
Th	0.310	0.132
U	0.309	0.128

values at Rennies River increased in the time period from 0 to 6 months and then decreased (Figure 4c). From this trend, there appears to be no relation between temperature and coating concentration. For Rennies River, dissolved oxygen trends were elevated after 3 months of coating accretion (Figure 4a), then decreased and thereafter reached a maximum concentration after 12 months of sampling. This should have produced elevated MnO_2 after 3 months, with a lower amount after 6 months of accretion, whereas the opposite was observed. The pH was relatively constant at sites SJS1, SJS6A, and SJS6B (Figure 4b) throughout the sampling period, with the difference between minimum and maximum values being less than one pH unit. Increased analyte concentrations after 3 months of coating accretion cannot be explained by pH.

Besides the stream water chemistry, the coating concentration trends may be due to some property of the Fe-Mn oxide coatings, such as crystallinity. Freshly precipitated Fe-Mn oxides are amorphous "gels," and then, as the coating ages, crystallization takes place (34). This results in the release of some adsorbed and coprecipitated metals because some ions do not fit into the crystal structure (42). Those that have a high

Table 5. Element concentrations determined by LA-ICP-MS in Fe-Mn oxide coatings present on pebbles (PEB) collected from the streambed and artificial substrates (SUB) located at site SWS1 in Rennies River, St. John's, NL.

	PEB	SUB	PEB	SUB	PEB	SUB	PEB	SUB
Month	3	3	6	6	9	9	12	12
Element								
V(ppm)	184	1810	543	566	243	495	1270	460
Cr(ppm)	185	5770	380	4100	28.9	445	2250	284
MnO ₂ (wt%)	73.3	17.3	66.1	68.4	68.5	74.3	41.4	63.5
Fe ₂ O ₃ (wt%)	20.5	74.4	28.0	23.4	26.0	22.6	54.5	33.7
Ni(ppm)	790	2600	857	3640	539	612	1810	291
Cu(ppm)	2590	15400	2390	10700	1540	3840	7100	1430
Zn(ppm)	20100	20500	18900	32800	15100	6200	5890	5330
Sr(ppm)	190	3230	1510	1180	173	326	496	166
Y(ppm)	471	1160	708	1160	574	434	547	367
Ba(ppm)	6510	19000	13100	14600	10100	12900	8780	10200
Ce(ppm)	2580	2030	1860	1110	1660	893	1230	1310
Pb(ppm)	8480	1890	4700	1900	6860	441	1430	712
Bi(ppm)	2.30	6.64	1.21	4.85	1.18	1.33	1.43	0.40
Th(ppm)	13.3	123	24.8	37.3	15.9	17.4	37.4	6.9
U(ppm)	5.39	43.1	12.6	58.7	6.40	18.0	13.7	8.26

probability of being excluded during crystallisation are those that have ionic radii that are unable to undergo isomorphous substitution in the newly formed Fe-Mn oxide coating. This may be occurring in this study, but Trivedi and Axe (41) found that crystallization did not occur in artificial amorphous iron and manganese oxides until after 6 months. Also, since MnO₂ and Fe₂O₃ are still being added in significant amounts, the amount of amorphous Fe-Mn oxide coating would remain high.

Iron-manganese oxide coatings can also contain significant amounts of organic material. For the samples from Rennies River, the amount increased with time, and this has the ability to block the coating from adsorbing metals from solution (34). This may account for the low concentrations found after 9 and 12 months. Organic matter can also cause a reduction of iron and manganese by lowering the Eh and pH; MnO₂ will dissolve at a higher Eh and pH than Fe₂O₃ (39). This did not occur here because MnO₂ coating amounts increased with time.

Table 6. Pearson-R correlation coefficients between analyte water and Fe-Mn oxide coating concentrations for samples taken from all sites in Rennies River.

Element	Mature coating	Fresh coating
V	0.032	-0.195
Cr	0.637	-0.583
Mn	-0.627	-0.507
Fe	0.756	0.434
Ni	0.037	-0.063
Cu	-0.566	-0.603
Zn	-0.118	-0.426
Sr	-0.492	-0.508
Y	NA	NA
Ba	-0.572	-0.732
Ce	-0.181	-0.342
Pb	-0.402	-0.739
Bi	-0.026	-0.269
Th	NA	NA
U	0.037	-0.334

Mature versus fresh Fe-Mn oxide coatings

Iron-manganese oxide coatings present on pebbles taken from the streambed are described as “mature” coatings, whereas coatings that accumulated on artificial substrates are called “fresh.” After 3 months of coating accretion at site SJS1, concentrations from the “fresh” coatings were higher than the “mature” coatings for all elements except MnO₂, Ce and Pb (Table 5). For the 6 and 9 month samples, more elements from the “mature” coatings had concentrations close to or greater than the “fresh” oxides. After 12 months of coating accretion, all of the elements except MnO₂, Ba, and Ce had greater concentrations in the “mature” coatings than in the “fresh” coatings, although the Ba and Ce “mature” concentrations were only slightly below the “fresh” concentrations. Similar trends were obtained for samples taken at the other sites. Depth profiles were examined to determine if the substrate was contributing other elements. It was found that the Fe-Mn oxides concentrated the analytes very well and that the substrate had no significant contribution to the analyte concentrations.

Pearson correlation coefficients were calculated

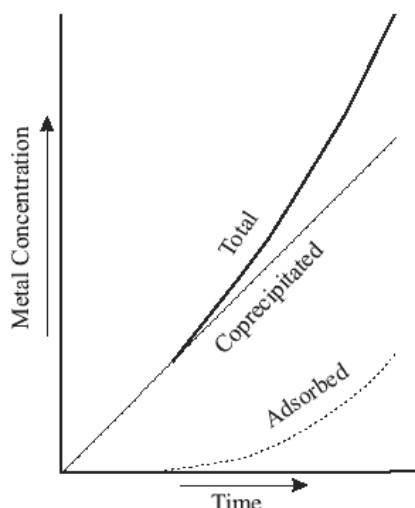


Figure 6. Diagram modified from Robinson (3) that illustrates the proposed model for trace metal scavenging by Fe-Mn oxides in a stream.

between element concentrations in the water samples and those in the “mature” and “fresh” Fe-Mn oxide coatings with the goal of defining which coating reflected water concentrations. All of the elements except Fe had negative correlation coefficients for the “fresh” coatings (Table 6). Fewer elements in the “mature” Fe-Mn oxide coatings had negative coefficients, and the relationships were low, whereas for the “fresh” coatings there were a lot of moderate negative relationships. Neither of the coatings appeared to represent stream analyte concentrations well, although the “mature” coatings may be considered slightly better.

Metal accumulation

Since the element concentration trends in the coating are not related to the stream chemistry of the sampling sites or properties of the coating, they must result from the metal accumulation process for Fe-Mn oxide coatings. The suggested process is shown in Figure 6 (3). Initial formation of Fe-Mn oxides on stream pebbles begins with precipitation of the Fe_2O_3 and MnO_2 phases; metals are precipitated along with this in a process called coprecipitation. Metals will initially coprecipitate with just Fe_2O_3 because there is no MnO_2 present, as it requires Fe_2O_3 nucleation sites. As the Fe-Mn oxides are precipitated, they begin adsorbing metals from solution. Initially, adsorption accounts for only a small amount of the metals present on the Fe-Mn oxide coating. As the coatings age, adsorption rates increase, thus leading to a

Table 7. Elements that loaded high in Factor 1 and Factor 2 for the annual accretion samples along with their common oxidation state in the environment, ionic radius and affinity.

Element	Factor	Oxidation state	Ionic radius (pm)	Affinity
V	1	5	49.5-68	Lithophile
Cr	1	6	58	Lithophile
Mn	2	4	53-67	Lithophile
Fe	2	3	63-92	Siderophile
Ni	1	2	63-83	Chalcophile
Cu	1	2	71-87	Chalcophile
Zn	1	2	74-104	Chalcophile
Sr	1	2	132-158	Lithophile
Y	1	3	104-121.5	Lithophile
Ba	2	2	149-175	Lithophile
Ce	1	3	115-148	Lithophile
Pb	1	2	112-163	Chalcophile
Bi	1	3	110-131	Chalcophile
Th	1	4	108-135	Lithophile
U	1	6	59-100	Lithophile

more rapid increase in metal accumulation. Adsorption also holds the property of increasing rates as the concentration of the given analyte increases in the stream (3). In summary, the total metal accumulation for Fe-Mn oxide coatings is a result of coprecipitation and adsorption.

At Rennies River, metal accumulation began with precipitation of mostly Fe_2O_3 at all sites during the first 3 months of coating accretion, as observed with elevated Fe_2O_3 amounts. The process of coprecipitation occurs during Fe_2O_3 precipitation, producing high concentrations of elements. Based on Figure 6 and Robinson's (3) model of metal accumulation, adsorption probably occurs only to a limited extent after 3 months of coating accretion.

The next part of the metal accumulation process begins with precipitation of a MnO_2 phase, which should be favoured on a fresh Fe_2O_3 surface. This occurs for the samples taken after 6 months of coating accretion (Group 3, Figure 2); evidence for the occurrence of this step is increased amounts of MnO_2 from 3 to 6 months. From 3 to 6 months, the mass of Fe-Mn oxide coating increases and its colour changes from a light brown staining,

indicating the increased amounts of Fe_2O_3 , to a darker colour due to higher amounts of MnO_2 . Elements also coprecipitate with the MnO_2 , but they do so to a lesser extent because all metal concentrations decrease, except for Ba, after 6 months of coating accretion. Barium has the largest ionic radius for all elements in both factors (Table 7), and it is possible that Ba is too large to fit into the coprecipitated structure of Fe_2O_3 but is able to fit into the MnO_2 structure. The actual mass of Fe-Mn oxide increases with time, but the ratio of metal to oxide coating decreases because lower quantities of metals are being coprecipitated with both oxides instead of only Fe_2O_3 . MnO_2 thus slows the coprecipitation of metals. This decrease in the rate of coprecipitated metal accumulation in the period from 3 to 6 months produces lower Fe-Mn oxide calculated concentrations, but the opposite occurs for Ba. These low concentrations indicate that adsorption is also at a minimum at this time.

The process of Fe_2O_3 and MnO_2 coprecipitation also occurs in the 9 and 12 month samples (group 4, Figure 2), as there are no major increases in coating concentrations, and the coatings appear larger and darker in colour. Some of the coating concentrations increase for the 12 month samples, and thus adsorption may be occurring at higher rates for these samples. Since the Pearson's-R correlation coefficients suggest that "mature" coatings represent stream chemistry better than "fresh" coatings, adsorption is low in these newly developed oxides.

Conclusions

Concentrations of a wide range of elements in Fe-Mn oxide coatings on "fresh" and "mature" coatings were determined using LA-ICP-MS after a suitable optimization of the instrumental operating parameters for this unique type of sample. The technique required minimal sample preparation, and the sample runs were relatively fast, with analysis times of 2 minutes.

Principal Component Factor Analysis was performed on the "fresh" Fe-Mn oxide coatings. Two factors were defined, and a graph of these showed four groupings which were based on location and the time at which the sampling took place. Coatings deposited in the initial 3 months of accretion were almost 100% Fe_2O_3 and contained elevated concentrations of various coprecipitated metals. Manganese oxide concentrations increased after 3 months and continued to increase for

the entire sampling period due to the affinity of manganese for the Fe_2O_3 surface. All the elements except Ba showed an interesting decrease in concentration with time, related to the low adsorption of most trace elements and low coprecipitation within the MnO_2 phase. Barium displayed a positive correlation with MnO_2 due to its large ionic radius. Adsorption rates further increased after 9 months of coating accretion.

The variables that govern element concentrations for "mature" coatings include element concentrations in the aqueous phase, dissolved oxygen levels, and pH values, but these variables do not appear important in controlling the concentrations in "fresh" coatings. This may be understood from the proposed model of accretion, wherein coprecipitation initially occurs and is predicted to continue for up to 3 years. Then adsorption starts at a low rate on the precipitated materials and increases exponentially until equilibrium with the stream environment is obtained. Trace element concentrations on "fresh" coatings are a result of both adsorption and coprecipitation, whereas on "mature" coatings, concentrations will primarily be caused by adsorption. Coprecipitation and adsorption affect element concentrations in different ways.

In order to make the results of this study conclusive, and to allow the PCFA to determine more than relationships between elements, more samples from each site are required. Sampling was limited in this study by both time and cost considerations. The different affinities of elements toward the MnO_2 and Fe_2O_3 phases also requires further investigation. Other factors that require examination are the effect of organic matter on metal accumulation and how the crystallinity of the oxide phase is related to adsorption. The processes of adsorption and coprecipitation appear complex, with a more lengthy study needed to address the time-frame and how element concentrations are affected by these processes.

References

1. G.A. Nowlan, *Journal of Geochem. Explor.*, **25**, 193 (1976).
2. P.R. Whitney, *Journal of Geochem. Explor.*, **4**, 251 (1975).
3. G.D. Robinson, *Chemical Geology*, **33**, 65 (1981).
4. L.H. Filipek, T.T. Chao and R.H. Carpenter, *Chemical Geology*, **33**, 45 (1981).
5. M. Thompson, M. Hale and B. Coles, *Trans.*

- Instn. Min. Metall. (Sect. B.: Appl. earth sci.)*, **101**, 9 (1992).
6. R.H. Carpenter and W.B. Hayes, *J. Geochem. Explor.*, **33**, 31 (1978).
 7. R.H. Carpenter and W.B. Hayes, *Chemical Geology*, **29**, 249 (1980).
 8. R.H. Carpenter, T.A. Pope and R.L. Smith, *J. Geochem. Explor.*, **4**, 349 (1975).
 9. T.E. Cerling and R.R. Turner, *Geochim. Cosmochim. Acta*, **46**, 1333 (1982).
 10. B.L. Gulson, S.E. Church, K.J. Mizon and A.L. Meier, *Appl. Geochem.*, **7**, 495 (1992).
 11. D. Günther, I. Horn and B. Hattendorf, *J. Anal. Chem.*, **368**, 4 (2000).
 12. D.W. Coish, unpublished Honours Thesis, Memorial University of Newfoundland, St. John's, Newfoundland, Canada, 1993.
 13. D.W. Coish, unpublished M.Sc. Thesis, Memorial University of Newfoundland, St. John's, Newfoundland, Canada, 2000.
 14. M. Hale, M. Thompson and M.R. Wheatley, *J. Geochem. Explor.*, **21**, 361 (1984).
 15. H.P. Longerich, "Laser Ablation-ICP-MS in the Earth Sciences; Chapter 2: Chemometrics", Mineralogical Association of Canada Short Course Series, **29**, 2001.
 16. N.R. Catto and L. St. Croix, "Urban geology of St. John's, Newfoundland", GAC special paper 42, Geological Association of Canadian, St. Johns NF, 445, 1998.
 17. S.D. Love and R.C. Bailey, *Can. J. Zool.*, **70**, 1976 (1992).
 18. J.K. Friel, C.S. Skinner, S.E. Jackson and H.P. Longerich, *Analyst*, **115**, 269 (1990).
 19. H.P. Longerich, J.K. Friel, C. Fraser, S.E. Jackson and B.J. Fryer, *Can. J. Appl. Spectrosc.*, **36**, 16 (1991).
 20. S.A. Crowe, B.J. Fryer, I.M. Samson and J.E. Gagnon, *J. Anal. At. Spectrom.*, **18**, 1331 (2003).
 21. A.B.E. Rocholl, K. Simon, K.P. Jochum, F. Bruhn, R. Gehann, U. Kramar, W. Luecke, M. Molzahn, E. Pernicka, M. Seufert, B. Spettel and J. Stummeier, *Geostandards Newsletter*, **21**, 101 (1997).
 22. E.V. Achterbergh, C.G. Ryan, S.E. Jackson and W.L. Griffin. "Laser Ablation-ICP-MS in the Earth Sciences; Appendix 3: Data reduction software for LA-ICP-MS." Mineralogical Association of Canada Short Course Series, **29**, (2001).
 23. J.I. Drever, "The Geochemistry of Natural Waters," Second ed, Prentice Hall Inc., New Jersey, 1988.
 24. T.T. Chao, *J. Geochem. Explor.*, **20**, 101, (1984).
 25. K.B. Krauskopf and D.K. Bird, "Introduction to Geochemistry", Third ed. McGraw-Hill, Inc., New York, 1995.
 26. V.F. Taylor, unpublished M.Sc. Thesis, Memorial University of Newfoundland, St. John's, Newfoundland, Canada, 2001.
 27. B. Wyrzykowska, K. Szymczyk, H. Ichichashi, J. Falandysz, B. Skwarzec and B.S. Yamasaki, *J. Agricultural Food Chem.*, **49**, 3425 (2001).
 28. J.F. Hair, R.E. Anderson and R.L. Tatham, "Multivariate Data Analysis", Second ed., Macmillan Publishing, New York, 1987.
 29. StatSoft, Inc, "Electronic Statistics Textbook", Tulsa, OK. (1999).
 30. A.W. Rose, H.E. Hawkes and J.E. Webb, "Geochemistry in Mineral Exploration," Second edition. Academic Press Inc., New York, 1979.
 31. Systat, "Statistics: Systat 6.0 for Windows". Chicago, Illinois. 1996.
 32. R.J. Ford, unpublished Honours Thesis, Memorial University of Newfoundland, St. John's, Newfoundland, Canada, 1992.
 33. P. Loganathan and R.G. Bureau, *Geochim. Cosmochim. Acta*, **37**, 1277 (1973).
 34. T. A. Jackson, "Environmental Interactions of Clays; Chapter 5: The Biogeochemical and Ecological Significance of Interactions Between Colloidal Minerals and Trace Elements", Springer, Berlin, 1998.
 35. P.K. Theobald Jr., H.W. Lakin and D.B. Hawkins, *Geochim. Cosmochim. Acta*, **27**, 121 (1963).
 36. J.J. Morgan and W. Stumm, *J. Colloid Sci.*, **19**, 347 (1964).
 37. P.R. Whitney, *J. Geochem. Exploration*, **4**, 251, (1975).
 38. J.D. Hem, *Chemical Geology*, **21**, 199 (1978).
 39. E.A. Jenne, *ACS Advances in Chemistry Series*, **73**, 337 (1968).
 40. C. Reimann and P. Caritat, "Chemical Elements in the Environment: Factsheets for the

Geochemist and Environmental Scientist”,
Springer, Berlin, 1998.

41. P. Trivedi and L. Axe, *Environ. Sci. Technol.*,

34, 2215 (2000).

42. D.G. Waslenchuk, *Environ. Geol.*, **1**, 131 (1975).